

Antibiotic-Loaded Chitosan Hydrogel with Superior Dual Functions: Antibacterial Efficacy and Osteoblastic Cell Responses

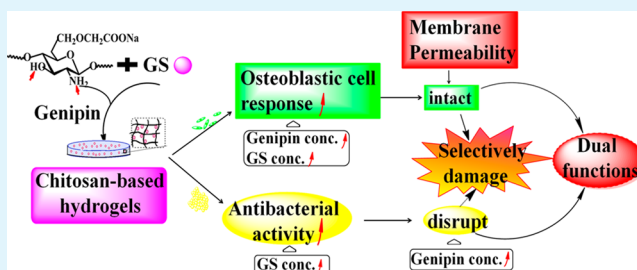
Fang Wu, Guolong Meng, Jing He, Yao Wu, Fang Wu,* and Zhongwei Gu

National Engineering Research Center for Biomaterials, Sichuan University, Chengdu 610064, P.R. China

S Supporting Information

ABSTRACT: It is critical for the clinical success to take the biological function into consideration when integrating the antibacterial function into the implanted biomaterials. To this aim, we prepared gentamycin sulfate (GS)-loaded carboxymethyl-chitosan (CM-chitosan) hydrogel cross-linked by genipin. The prepared hydrogels not only achieved superb inhibition on bacteria growth and biofilm formation of *Staphylococcus aureus* but also significantly enhanced the adhesion, proliferation, and differentiation of MC3T3-E1 cells. The observed dual functions were likely based on the intrinsic property of the positive charged chitosan-based hydrogel, which could be modified to selectively disrupt the bacteria wall/membrane and promote cell adhesion and proliferation, as suggested by the membrane permeability study. The genipin concentration played an important role in controlling the degradation time of the chitosan hydrogel and the MC3T3-E1 cell responses. The loading of GS not only significantly increased the antibacterial efficiency but also was beneficial for the osteoblastic cell responses. Overall, the biocompatibility of the prepared chitosan-GS hydrogel could be tuned with both the genipin and GS concentrations, which control the available positive charged sites of chitosan. The results demonstrated that chitosan-GS hydrogel is an effective and simple approach to achieving combined antibacterial efficacy and excellent osteoblastic cell responses, which has great potential in orthopedic applications.

KEYWORDS: carboxymethyl chitosan, gentamycin sulfate, hydrogel, biofilm, membrane permeability



1. INTRODUCTION

Biomaterial-related infection has remained a serious problem for clinical applications, especially due to the formation of biofilms on the implanted biomaterials.^{1–3} Accordingly, there has been increasing attention on developing antibacterial materials to defend against infections. However, another important issue needs to be considered in biomaterial design is the osseointegration of the medical implants. Unfortunately, the introduction of the antibacterial ingredients into the medical device is often associated with the adverse effect on host cells and the compromise of its biological functions. Designing materials to fulfill the requirement for antibacterial and biocompatibility thus has been a challenging task.

For instance, Ag⁺ has received widespread recognition due to its broad spectrum antimicrobial property and the best antibacterial efficacy among various metal ions,^{4,5} but it would likely have a detrimental effect on the cell response and even could be potentially toxicological at high concentrations.^{4,6} Another approach is to use antibacterial polymer coatings that are highly compatible. Although toxicity has remained a critical issue for most polymer-based coatings,^{7–9} impressive selectivity against bacteria has been reported with some cationic polymers and peptides.^{10–13} Nevertheless, the best achieved so far is just to minimize the cytotoxicity, let alone to improve the biocompatibility of the biomaterials despite all the scrupulous efforts made on the polymer design.

The alternate approach to increasing the osteogenic functions is to incorporate Arg-Gly-Asp peptide (RGD) or growth factors into the antibacterial materials that would enhance cell response.^{14–16} However, these methods tend to be complicated and costly.

Among all the antibacterial materials, chitosan and its derivative have demonstrated both antibacterial properties and biocompatibility and have been widely used in orthopedic applications and drug delivery carriers.^{17–21} As a natural polysaccharide, chitosan possesses intrinsic antibacterial property because of its cationic amino group that interrupts the bacterial membrane and disrupts the mass transport across the bacterial wall.^{19,22} On the other hand, chitosan-based materials have also been reported to improve the cell adhesion and proliferation.^{23,24} Although the antibacterial efficacy of chitosan-based biomaterials depends on the parameter of chitosan, including molecular weight, degree of deacetylation, and the concentration of chitosan solution,^{22,25–27} these material parameters also affect the cell compatibility.²¹

We previously hypothesized that the chitosan-based material might be tuned to achieve dual functions of antibacterial efficiency and osteogenic activity through selectively interrupt-

Received: December 19, 2013

Accepted: June 18, 2014

Published: June 18, 2014

ing the bacteria membrane. This phenomenon was substantiated by selecting a water-soluble chitosan derivative within a specific concentration window, which promoted the osteoblast-like cell proliferation and invaded the bacteria membrane simultaneously.²⁵ However, the antibacterial efficiency was significantly compromised to entertain the requirement for cell biocompatibility. In addition, such chitosan material was in film form which was subjected to quick degradation.²⁵ To overcome the above shortcomings, we have adopted a simple scheme in this study by preparing chitosan hydrogels with antibiotic loading, to achieve controlled and sustained release of the antibacterial ingredients and antibacterial efficiency at longer terms. Antibiotics are routinely administered at the first couple of days in implant surgery operations generally through the vascular injection. The local release of the antibacterial ingredient at the surgical sites is highly desirable in implant applications.^{28–30} Among various antibiotics, gentamycin sulfate (GS) has been used to treat deep bone infections by virtue of its excellent performance against microorganism combined with advantages of low cost, broad antibacterial spectrum of action, low allergy rate, good stability, and good water solubility.^{30–32} It targets against the synthesis of bacterial protein with little detrimental effect on cell responses.

In the present work, the carboxymethyl-chitosan (CM-chitosan) hydrogel was prepared by using genipin as the cross-linking agent, with the additional incorporation of gentamycin sulfates (GS) to enhance its antimicrobial activity. *Staphylococcus aureus* (*S. aureus*), a common pathogen in the osteomyelitis and cardiovascular implant infections, was selected to systematically test the antibacterial efficacy of the prepared materials, in terms of bacteria growth and biofilm formation. MC3T3-E1 cells were used to test the osteogenic activity of the prepared chitosan-GS hydrogels in terms of cell adhesion, proliferation and differentiation. In particular, an attempt has been made to investigate if there was a selective disruption effect of the prepared materials on cell/bacterial membranes, and thus provide insight into understanding the dual functions of the prepared chitosan-GS hydrogels.

2. EXPERIMENTAL SECTION

2.1. Materials. Carboxymethyl-chitosan (Carboxylation degree $\geq 80.0\%$ and MW = 1×10^5) was purchased from Aoxing Biotech (Zhejiang, China). Genipin was obtained from Linchuan Zhixin Biotech (Fuzhou, China), which has been derived from *Gardenia jasminoides* Ellis geniposide. Gentamycin sulfate (GS) was purchased from Ameresco (Solon, Ohio, USA). Phosphate buffered saline (PBS), methyl thiazolyl tetrazolium (MTT), dexamethasone, β -glycerophosphate ascorbic acid, triphosphopyridine nucleotide (TPN), and glucose-6-phosphate were obtained from Sigma-Aldrich.

2.2. Hydrogel Preparation. Before preparation, the CM-chitosan powder was sterilized by treating with γ -radiation from cobalt-60 sources (Sichuan Atomic Physical Research Institute, Sichuan, China). The aqueous genipin solution was sterilized by filtering with 0.22 μm syringe filters. CM-chitosan-GS hydrogel were prepared by adding 1 mL of freshly prepared GS aqueous solution (20 mg/mL) and then 1 mL of genipin solution (with various concentrations) to 20 mL of CM-chitosan aqueous solution (50 mg/mL) aseptically, unless specified otherwise. The genipin concentrations were chosen according to the weight ratio of genipin to CM-chitosan at 0.5%, 1%, 2%, respectively. The GS to hydrogel ratio was kept constant at 1 mg/mL as indicated above for all bacterium and cell experiments, except for the experiments in section 2.7 where various GS concentrations were used. These homogeneous solutions were kept under sterilized condition at 37 °C for 24 h. Finally, three kinds of

hydrogel complexes were formed and would be referred as chitosan-0.5% genipin, chitosan-1% genipin, and chitosan-2% genipin. All solutions are aqueous solutions unless specified otherwise.

2.2.1. Characterization Studies. Digital photos of the three hydrogel complexes before and after gelation were taken by Nikon camera (COOLPIX S70, Japan). The relevant reaction was analyzed by UV-vis spectrophotometer (UV-2100, Shimadzu, Japan) (see Figure S1 in the Supporting Information).

2.2.2. In Vitro Release of the GS. Chitosan-0.5% genipin, chitosan-1% genipin and chitosan-2% genipin were used to examine the in vitro release behavior of the antibiotics from the prepared hydrogel. The hydrogel samples (0.5 mL for each sample, with a GS to hydrogel ratio of 1 mg/mL) were placed into the centrifugal tubes containing 16 mL Phosphate buffered saline (PBS) solution (pH 7.4) and then incubated at 37 °C under shaking at a rate of 100 rpm. One mL of the solution was withdrawn at various time points of 1, 2, 4, 8, 12, 24, 48, 96, 144, 240, 336, and 504 h, and stored at 4 °C before analysis by UV-vis spectrophotometer (UV-2100, Shimadzu, Japan) using the o-phthalaldehyde method at 332 nm.³³

2.3. Bacterial Inhibition. Before gelation, GS-loaded CM-chitosan hydrogel samples (0.5 mL for each sample, with a GS to hydrogel ratio of 1 mg/mL) at different genipin concentrations (0.5, 1, and 2%) were introduced into 24-well plates and then allowed gelation for 24 h. The tissue culture plates were served as control. After that, 1 mL suspension of the *Staphylococcus aureus* (ATCC 25923) were spread onto the hydrogel materials with an initial bacterial density of $1-2 \times 10^6$ CFUs/mL. The final GS concentration was about 300 $\mu\text{g}/\text{mL}$ in terms of total volume (about 0.45 mg of GS in 0.5 mL of hydrogel and 1 mL of culture medium). The medium was changed every 2 days in the experiment. The MTT assay was selected for evaluating bacterial inhibition at 1, 3, 5, 7, and 14 days, respectively. After incubation for 1, 3, 5, 7, and 14 days, 200 μL MTT solution (5 $\mu\text{g}/\mu\text{L}$ in PBS) was added to each well and incubated for another 4 h. Removing the supernatant carefully, 1 mL of dimethyl sulfoxide (DMSO) was then added into each well to dissolve the purple formazan. After gentle mixing for 5 min with an oscillator, the optical density (OD) values obtained at 490 nm were related with the living bacterial.

After 5 days of culture, the samples were treated with 2.5% glutaraldehyde, dehydrated by a graded series of ethanol, dealcoholized by a graded series of isoamyl acetate and subjected to critical point drying. Afterward, the morphologies of *S. aureus* were examined by the scanning electron microscope (SEM, S4800, Hitachi Ltd., Tokyo, Japan).

2.4. Biofilm Inhibition. Nikon digital camera had been used to observe the bacterial colony macroscopically. The *S. aureus* were seeded onto 35 mm glass-bottom culture dishes (NEST Biotech, China) containing the three different hydrogel complexes (with a final GS concentration of 300 $\mu\text{g}/\text{mL}$), with the blank culture dishes as control. All samples were subjected to incubation at 37 °C, and digital photos were taken at the prescribed 1, 3, 5, 7, and 14 day incubation times, respectively.

2.5. Osteoblastic Cell Responses. Prior to gelation, the GS-loaded CM-chitosan hydrogel samples (0.1 mL for each sample, with a GS to hydrogel ratio of 1 mg/mL) were transferred to new wells in 24-well plates that were either empty or with hydroxyapatite (HA) coating, respectively. After gelation, 1 mL suspension of MC3T3-E1 cells with number 20 000 per well was seeded onto the hydrogel surfaces under a humidified atmosphere with 5% CO₂ at 37 °C for 3, 5, and 7 days, with the tissue culture plates as control. The MC3T3-E1 cells were maintained in the culture medium which contained 1 mL of α -MEM (HaLi Corporation, Chengdu, China) supplemented with 10% fetal bovine serum (FBS, HyClone, Thermo Fisher Scientific Inc., USA). For osteogenic induction, the MC3T3-E1 cells were cultured at 1, 3, 5, and 7 days in the osteogenic induction medium (the induction medium consisted of α -MEM, 10% FBS, 0.1 $\mu\text{mol}/\text{L}$ of dexamethasone, 10 mmol/L of β -glycerophosphate, and 50 $\mu\text{mol}/\text{L}$ of ascorbic acid)³⁴ (see Figure S3 in the Supporting Information). SEM was used to examine the cell morphology at 5 d culture. The cell proliferations on the three hydrogel samples were determined by the MTT assay. The N-Cadherin, runt-related transcription factor-2 (Runx2), alkaline

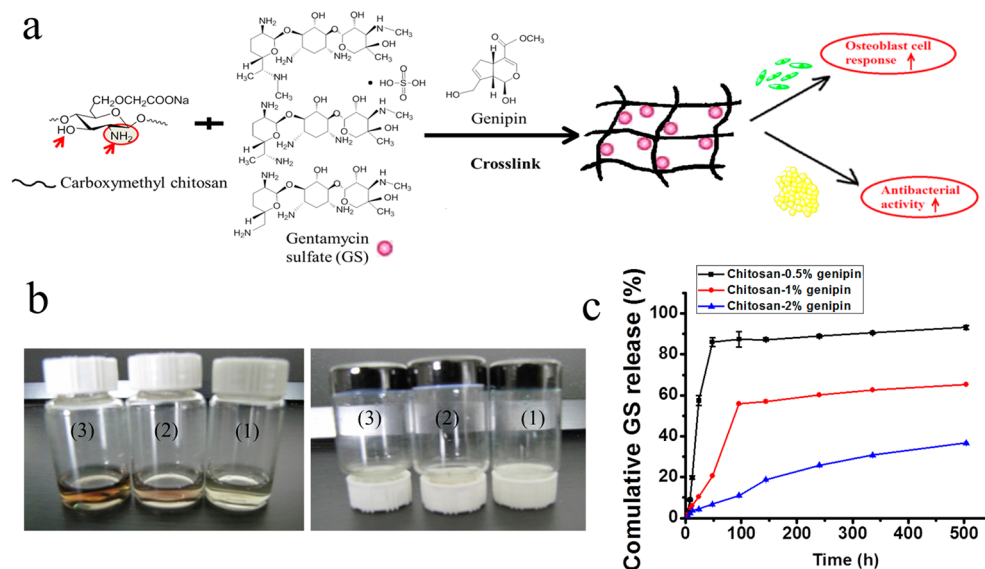


Figure 1. Preparation and characterization of the chitosan-GS hydrogel. (a) Schematic drawing of the preparation of the chitosan hydrogel. (b) Photographs of chitosan-0.5% genipin (1), chitosan-1% genipin (2), and chitosan-2% genipin (3), left: before the formation of hydrogel, and right: after the formation of hydrogel. (c) Release of GS from chitosan-0.5% genipin, chitosan-1% genipin, and chitosan-2% genipin (with a GS to hydrogel ratio of 1 mg/mL) as a function of time.

phosphatase (ALP) activity were determined using the quantitative enzyme-linked immunosorbent assay (ELISA) after 1, 3, 5, 7 days. The protein expressions were measured according to the instructions of the ELISA kits (ColorfulGene, Colorfulgene Biological Ltd., Wuhan, China) by the absorbance at 450 nm with a spectrophotometer (MK3, Thermo Electron Ltd., USA), compared against a calibration curve produced using a set of standard samples.

2.6. Effect of the Prepared Hydrogels on Membrane Permeability. **2.6.1. Permeability of the *S. aureus* Wall/Membrane.** Membrane permeability was determined by the leakage level of cytoplasmic materials in the culture as a result of disruption of the bacterial wall/membrane. Similar to the bacteria inhibition studies in section 2.3, 1 mL of suspension of the *S. aureus* (with an initial bacterial density of $1-2 \times 10^6$ CFUs/mL) were spread onto 0.5 mL GS loaded CM-chitosan hydrogels (at different 0.5%, 1% and 2% genipin concentrations) with a final GS concentration of 300 μ g/mL, using tissue culture plates as control. At the end of 6 h, 12 h, 1 day, and 3 days of culturing, a 0.2 mL aliquot of the *S. aureus* suspension was taken out for leakage analysis.

Alkaline phosphates (ALP) were measured according to the method described in the previous literature.²² The reaction mixture was 0.1 mg of *p*-nitrophenylphosphate in 0.5 M Tris-HCl buffer (pH 8) and the total volume was 1 mL. The reaction was analyzed by the UV-vis spectrophotometer, and the optical density of the suspension at 420 nm was measured. The amount of enzyme that produced 1 μ M of *p*-nitrophenylphosphate in 1 min at 28 °C was deemed as a unit of released ALP activity.

Glucose-6-phosphate dehydrogenase (G6PDH) activity was also measured through the method described by the literature.²² There was 0.05 M Tris-HCl (pH 8), 0.01 M CaCl₂, 1.0 μ M glucose-6-phosphate and 0.4 μ M triphosphopyridine nucleotide (TPN) in the reaction solution (total volume: 1 mL). The product was detected by the UV-vis spectrophotometer at 340 nm. The amount of enzyme that reduced 1 μ M of TPN-equivalent in 1 min at 28 °C was deemed as a unit of released G6PDH activity.

The detection of absorbance at 260 nm (A260) was linearly associated with the leakage of nucleic acid.³⁵ The suspension was withdrawn and filtered with 0.22 μ m syringe filters to remove the bacteria. Then, the optical density at 260 nm was detected by UV-vis spectroscopy.

2.6.2. Permeability of the MC3T3-E1 Cell Membrane. Cell membrane permeability studies were carried out using the procedures similar to the osteoblastic cell response studies in section 2.5. Lactate

dehydrogenase (LDH) in culture medium was measured to indicate the disruption of the cell membrane, using the quantitative enzyme-linked immunosorbent assay (ELISA). All the procedures were strictly conducted according to the protocols of the ELISA LDH test kit (ColorfulGene, Colorfulgene Biological Ltd., Wuhan, China). The leakage were determined by the absorbance at 450 nm with a spectrophotometer (MK3, Thermo Electron Ltd., USA), compared against a calibration curve produced using a set of standard samples.

At the end of 6 h and 3 days of inoculating, the MC3T3-E1 cells were examined under a confocal laser scanning microscope (CLSM, Olympus IX 95). Before observation, the supernatant was discarded and washed twice by PBS, and then stained by fluorescein diacetate (FDA) and propidium iodide (PI), for live and dead cells, respectively.

2.7. Effect of Antibiotic (GS) Concentration on Antibacterial Efficiency and MC3T3-E1 Cell Proliferation. The CM-chitosan-2% genipin hydrogel was selected to test the effect of GS concentration on antibacterial efficacy and MC3T3-E1 cell proliferation. The chitosan-GS hydrogels were prepared in the same method previous described in section 2.2, but with different GS concentrations. The ratios of GS to hydrogel were 3.3, 16.5, 33, 66, 165, 330, and 1000 μ g/mL, respectively and would be referred as chitosan-GS (1), chitosan-GS (2), chitosan-GS (3), chitosan-GS (4), chitosan-GS (5), chitosan-GS (6), and chitosan-GS (7), respectively. Both tissue culture plates and CM-chitosan-2% genipin hydrogel without GS loading were selected as control.

The bacteria inhibition and cell response studies were carried out with procedures similar to those in sections 2.3 and 2.5, respectively. In brief, for antibacterial efficiency, 1 mL of the bacterial suspension containing $1-2 \times 10^6$ CFUs/mL were incubated on the prepared hydrogels (0.5 mL for each sample) or blank culture plates for 1, 3, 5, and 7 days, respectively. The above hydrogel complexes had the corresponding final GS concentrations in bacteria media of 1, 5, 10, 20, 50, 100, and 300 μ g/mL, respectively. For cell response study, 1 mL of MC3T3-E1 cells suspension (2×10^4 cells/mL) was inoculated on the hydrogel materials (0.1 mL for each sample) for 1, 3, 5, and 7 days, respectively. MTT assay was selected for evaluating the bacterial inhibition as well as MC3T3-E1 cell proliferations with the optical density (OD) values at 490 nm.

2.8. Statistical Analysis. All experiments were carried out as means \pm standard deviation for $n = 3$. The one-way ANOVA test was utilized to examine the significant differences between the various groups. All tests were carried out by SPSS and a $p < 0.05$ suggested the presence of significant difference.

3. RESULTS

3.1. Hydrogel Characterization. A schematic drawing of the preparation of chitosan-GS hydrogel is given in Figure 1a. The addition of the cross-linking agent genipin to CM-chitosan/GS solutions resulted in color change, and the three materials (chitosan-0.5% genipin, chitosan-1% genipin, and chitosan-2% genipin) showed slightly yellow color prior to gelation (Figure 1b). The color became darker as the genipin's concentration increased, suggesting possible reactions between the genipin and chitosan/GS as genipin would react with the amino groups of both compounds. New absorption peaks have observed in the spectra of chitosan-genipin, GS-genipin, and chitosan-GS-genipin complexes, respectively (see Figure S1 in the Supporting Information), indicating the genipin's reactions with both chitosan and GS and the formation of the corresponding new compounds. After gelation, all three samples turned a bluish color.

As shown in Figure 1c, the bound antibiotics released fast from the chitosan-0.5% genipin hydrogel at the first 2 days and about 93.2% of the total incorporated antibiotic had been released from the hydrogel in 21 days. However, about 65.2 and 36.7% of the antibiotic were respectively released from the chitosan-1% genipin and chitosan-2% genipin within 21 days, which are much lower than that from the chitosan-0.5% genipin. The results overall were not surprising because the degree of cross-linking would affect the release behaviors. All these hydrogels had good fitting with Korsmeyer-Peppas model, and the fitting results indicated a Super Case-II transport mechanism for chitosan-0.5% hydrogel and non-Fickian diffusion mechanism for chitosan-1% and chitosan-2% hydrogels. More detailed analysis of the release kinetics of the three hydrogels was given in the Supporting Information (Table S1).

3.2. Antibacterial Activity. The bacterial inhibition was examined through the MTT assay after a suspension of *S. aureus* bacteria being cultured on three hydrogel materials for 1, 3, 5, 7, and 14 days. As shown in Figure 2a, the OD values of all three samples were at least 1 order of magnitude lower than those of control at any given time, suggesting that all prepared materials exhibited good antibacterial activities. There were no obvious differences in OD values of the three chitosan-GS complexes (Figure 2a), whereas the antibacterial activity increased weakly with the decrease of genipin concentration

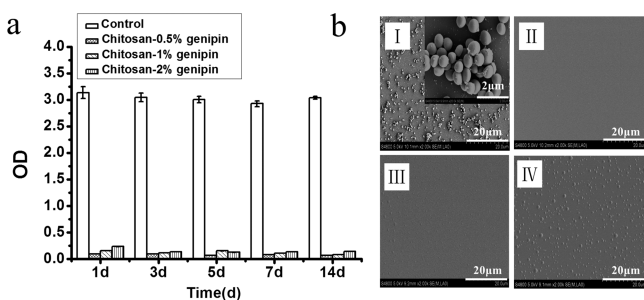


Figure 2. Bacterial inhibition of three different chitosan-GS hydrogel materials (with a final GS concentration of 300 $\mu\text{g}/\text{mL}$ in total media), with the tissue culture dishes as control. (a) MTT result of *S. aureus* cultured on three different materials at 1 d, 3 d, 5 d, 7 d, 14 d. (b) SEM micrographs of *S. aureus* culture on different material surfaces at 5 days. I, Control; II, chitosan-0.5% genipin; III, chitosan-1% genipin; IV, chitosan-2% genipin. Error bars represent standard deviation of the mean for $n = 3$.

and the chitosan-0.5% genipin sample exhibited the best bacteria inhibition. The small difference in antibacterial activities was likely due to the different release behaviors previously observed for the three hydrogel samples. SEM micrographs showed the morphology of *S. aureus* after 5 days of culture on the surfaces of the control, chitosan-0.5% genipin, chitosan-1% genipin, and chitosan-2% genipin, respectively (Figure 2b). No bacteria were observed on the prepared samples, which was in good agreement with the MTT observations.

3.3. Biofilm Inhibition. Prevention of bacteria adhesion and biofilm formation is critical to defending biomaterials-related infections. The antibiofilm efficiency was analyzed by examining the formation of the bacterial colony on culture dishes with different prepared materials (Figure 3). Masses of

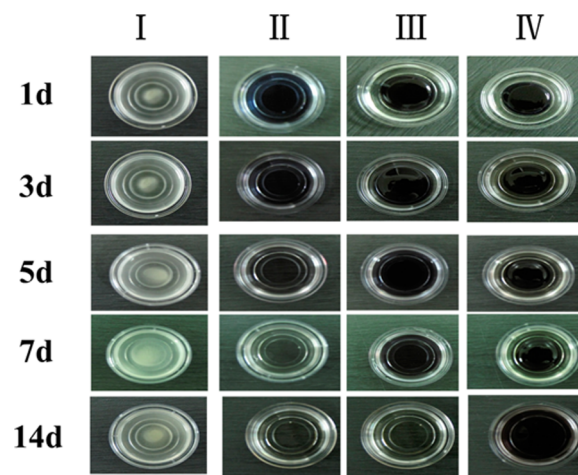


Figure 3. Optical photographs of *S. aureus* on the sample (with a final GS concentration of 300 $\mu\text{g}/\text{mL}$ in total media) for 1, 3, 5, 7, and 14 days (from top to bottom), with the blank culture dishes as control: I, control; II, chitosan-0.5% genipin; III, chitosan-1% genipin; and IV, chitosan-2% genipin (from the left to the right).

white sediments, i.e., the formation of biofilm, had been observed on the control surfaces throughout the culture periods. For all chitosan-GS samples, there was no such deposit observed at any given time points, indicating significant inhibition on biofilm formation. Meanwhile, physical degradation of the hydrogel structure had been observed to take place at 1, 5, and 14 days in the chitosan-0.5% genipin, chitosan-1% genipin, and chitosan-2% genipin samples, respectively.

3.4. Osteoblastic Cell Responses. MC3T3-E1 cells adhered and spread on all surfaces, but difference in cell morphology, cell numbers and cell adhesion were observed between chitosan hydrogels and the blank control. The SEM observations showed enhanced cell adhesion and proliferation on the hydrogel samples (Figure 4a and Figure S2 in the Supporting Information). Overall, all chitosan hydrogel samples show enhanced N-cadherin expressions compared with the control. In particular, significant higher expressions of N-Cadherin were observed on the chitosan-2% genipin samples (Figure 4b) than those on the control at all times (1, 3, 5, 7 days), indicating robust cell-matrix interactions. The MTT results further confirmed the SEM observations. As shown in Figure 4c, when placed on empty culture wells, all chitosan hydrogels showed higher OD values than that of the control and the chitosan-2% genipin sample had the highest OD values.

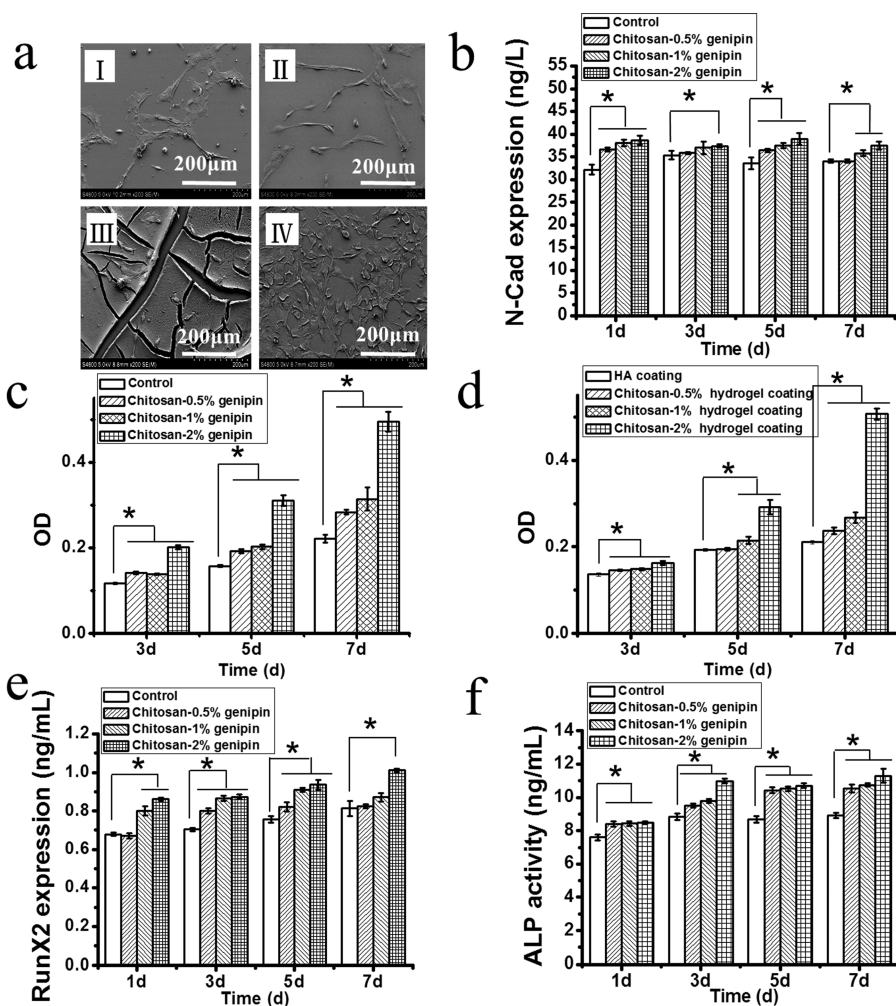


Figure 4. Effect of the chitosan hydrogels on the osteoblastic cell response, with the tissue culture dishes as control. (a) SEM micrographs of MC3T3-E1 cultured on different sample surfaces after 5 days. I, control; II, chitosan-0.5% genipin; III, chitosan-1% genipin; IV, chitosan-2% genipin. (b) adhesion-related protein (N-cadherin) expressions of MC3T3-E1 cells on control, chitosan-0.5% genipin, chitosan-1% genipin, and chitosan-2% genipin for 1, 3, 5, and 7 days. Proliferations of MC3T3-E1 cells cultured on control, chitosan-0.5% genipin, chitosan-1% genipin and chitosan-2% genipin for 3, 5, and 7 days. (c) in the absence of HA coating. (d) on HA coating surfaces. Differentiation-related expressions of MC3T3-E1 cells on control, chitosan-0.5% genipin, chitosan-1% genipin, and chitosan-2% genipin for 1, 3, 5, and 7 days. (e) RunX2; (f) ALP. Error bars represented standard deviation of the mean for $n = 3$ ($*p < 0.05$ vs control as statistically significant).

This suggested that the prepared hydrogels had excellent biocompatibility. Same experiments were carried out by placing the chitosan samples on the HA coating surfaces due to their intended usages in load-bearing applications. Similar trend was observed for the cell proliferation when the prepared hydrogel were placed on the HA coating surface (Figure 4d). The expressions of Runx2 and ALP (Figure 4e, f) were measured to analyze the osteoblastic cell differentiation. The CM-chitosan hydrogel samples showed higher Runx2 and ALP expression, demonstrating enhanced osteogenic differentiation (Figure 4e, f). Overall, the results clearly demonstrated that the prepared materials not only showed little cytotoxicity, but also enhanced the osteogenic activity. In particular, the MC3T3-E1 cells had the best spreading (Figure 4a and Figure S2 in the Supporting Information), proliferation (Figure 4c, d and Figure S2 in the Supporting Information) and differentiation (Figure 4e, f) on the chitosan-2% genipin samples.

The osteoblastic differentiation course was also carried out by culturing the MC3T3-E1 cells with the osteogenic induction medium (see Figure S3 in the Supporting Information). Overall, similar trend has been observed for the cell adhesion,

proliferation and differentiation of MC3T3-E1, but with a clearer upward trend of the OD values and protein expressions with the increase of the genipin concentration (degree of cross-linking) and significantly enhanced osteoblastic cell response over the control for all three genipin concentrations. The results also demonstrated a significantly stronger dependence of N-cad expressions on genipin concentration under osteogenic induction media, compared with the normal culture media used above.

3.5. Effect of the Prepared Hydrogels on Membrane Permeability. **3.5.1. Permeability of the *S. aureus* Wall/Membrane.** The leakages of enzyme and nucleotides from *S. aureus* were analyzed to indicate the damage of the bacterial wall or membrane (Figure 5). The enzyme levels of ALP and G6PDH (in association with the leakages of outer wall and membrane respectively²²) in all chitosan hydrogels were higher than those of the control (Figure 5a, b), indicating appreciable damages of bacterium wall and membrane at the presence of the chitosan-GS hydrogels. Similar trend has been found for nucleotide leakage, a direct indication of the disruption of bacteria membrane. A significant amount of 260 nm absorbing

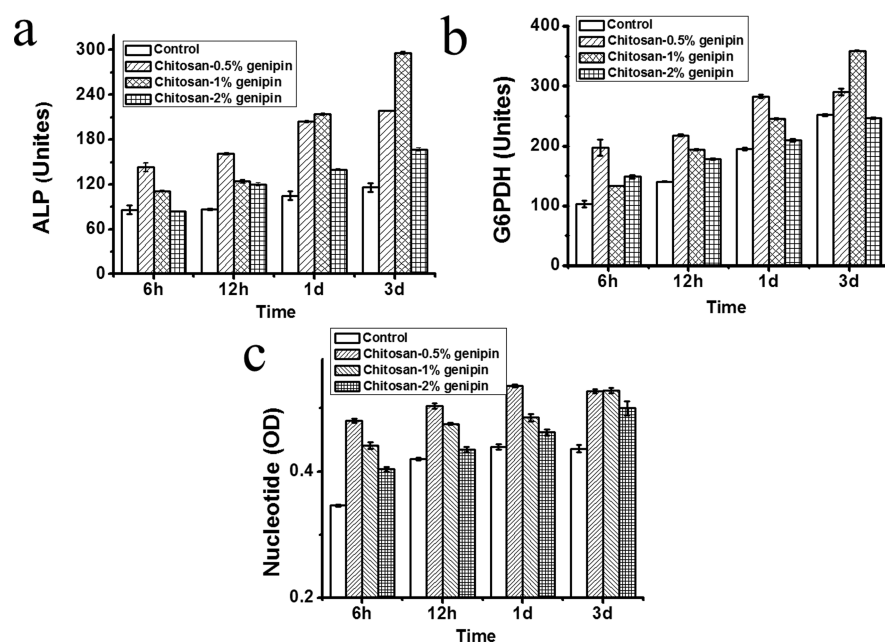


Figure 5. Effect of prepared hydrogels on the leakage of enzyme and nucleic acid from *S. aureus* for 6 h, 12 h, 1 day, and 3 days, with the tissue culture dishes as control. (a) ALP, (b) G6PDH, (c) nucleic acid. Error bars represent standard deviation of the mean for $n = 3$.

material has been observed in the presence of chitosan materials (Figure 5c), indicating a high-level leakage of nucleotides from *S. aureus*. Overall, the release of the cytoplasmic materials decreased as the genipin's concentration increased and the chitosan-2% genipin sample had the lowest enzyme and nucleotide leakages among all the chitosan materials.

3.5.2. Permeability of the MC3T3-E1 Cell Membrane. The LDH release in the media was used as an indication of the disruption of the osteoblastic cell membrane. The LDH concentrations in the medium for all chitosan hydrogel samples were significant lower than those of the control at 3 days, whereas a mixed trend were observed at 6 h. This might suggest a protective effect of CM-chitosan against the loss of membrane integrity (Figure 6a). It was also clear that the amounts of LDH released from the cells to the culture medium decreased with the increase of the genipin content. Figure 6b showed the fluorescence staining photos of the MC3T3-E1 cells cultured for 6 h and 3 d on the hydrogel surface. Most of the cells on the materials were round at 6 h, indicating that cells were not yet well adhered to the sample surface. However, abundant spindle-shaped cells can be observed at the end of the third day. No significant difference was observed between the cells on the chitosan materials and the blank control at 3 days, indicating that all chitosan hydrogel materials had excellent biocompatibility.

3.6. Effect of Antibiotic (GS) Concentration on Antibacterial Efficiency and MC3T3-E1 Cell Proliferation of Chitosan-GS Hydrogels. As shown in Figure 7a, the bacterial inhibition was significantly enhanced with the increasing GS concentration from 1 to 100 $\mu\text{g}/\text{mL}$ and almost remained unchanged above 100 $\mu\text{g}/\text{mL}$. Overall, the chitosan-GS hydrogel materials exhibited excellent antibacterial property throughout the culture time at high GS concentrations. More surprisingly, the cell proliferation also increased as GS concentration increased (Figure 7b).

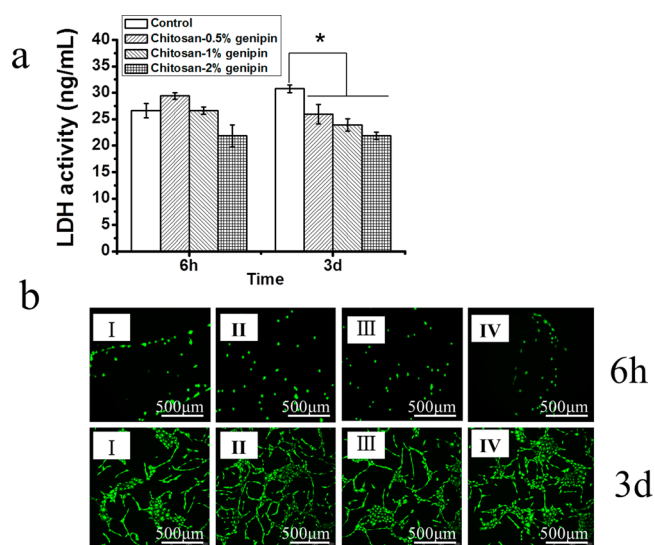


Figure 6. Effect of prepared hydrogels on the leakage of cell inclusions from MC3T3-E1 cells for 6 h and 3 days, with the tissue culture dishes as control. (a) LDH activities in the medium after the contact between the chitosan-based and MC3T3-E1 cells. (b) CLSM photos of MC3T3-E1 cells cultured on different sample surfaces. I, control; II, chitosan-0.5% genipin; III, chitosan-1% genipin; IV, chitosan-2% genipin. Error bars represent standard deviation of the mean for $n = 3$ (* $p < 0.05$ vs control as statistically significant).

4. DISCUSSION

To develop antibacterial materials without the compromise of the biological functions is critical for the clinical success of the implant device, especially in the orthopedic applications. However, it has been a challenging task so far, with very rare success reported.³⁶ To this aim, genipin cross-linked CM-chitosan hydrogel has been prepared with the further incorporation of antibiotics (GS), to achieve combined superior antibacterial efficacy and osteogenic activity.

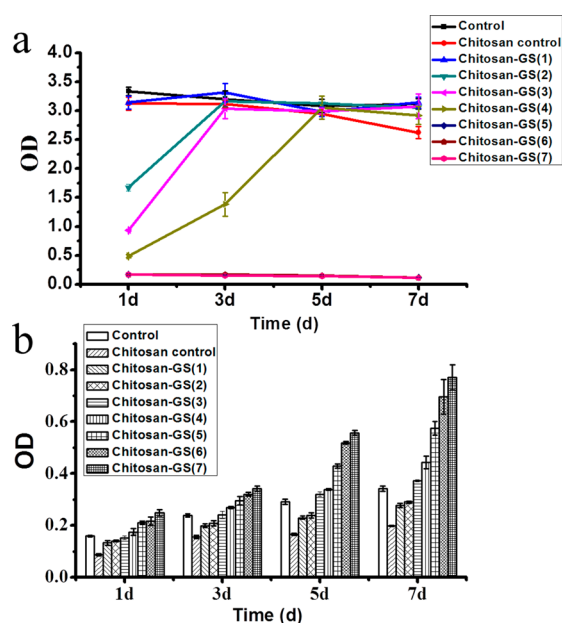


Figure 7. Effect of antibiotic (GS) concentration on antibacterial efficiency and MC3T3-E1 cell proliferation of chitosan-2% genipin-GS hydrogels, with the tissue culture dishes as control (a) *S. aureus* cultured on the control, chitosan control, chitosan-GS (1), chitosan-GS (2), chitosan-GS (3), chitosan-GS (4), chitosan-GS (5), chitosan-GS (6), and chitosan-GS (7) for 1, 3, 5, and 7 days. (b) MC3T3-E1 cells cultured on the control, chitosan control, chitosan-GS (1), chitosan-GS (2), chitosan-GS (3), chitosan-GS (4), chitosan-GS (5), chitosan-GS (6), and chitosan-GS (7) for 1, 3, 5, and 7 days. The medium was half-changed every 2 days. Error bars represent standard deviation of the mean for $n = 3$.

The prepared chitosan-GS hydrogels demonstrated excellent antibacterial ability with significantly reduced bacteria growth (Figure 2a, b) and strong inhibition against biofilm formation of *S. aureus* (Figure 3). Both CM-chitosan and antibiotics would contribute to the observed superb antibacterial efficacy but with a more predominant contribution from the antibiotics (GS). Variation of the genipin content (0.5, 1.0, and 2.0%) had less impact on the antibacterial efficacy compared to the total reduction of bacteria count of more than 1 order of magnitude rendered by the chitosan/antibiotic system (Figure 2a).

It was encouraging to notice that the prepared chitosan-GS hydrogel promoted the adhesion, proliferation and differentiation of the MC3T3-E1 osteoblast cells (Figure 4a–f, and Figure S3 in the Supporting Information). Better cell adhesion has been observed on chitosan-GS hydrogels (Figure 4a). The N-cadherin measurement also suggested increased cell-matrix interactions on chitosan-GS surfaces (Figure 4b and Figure S3 in the Supporting Information). The OD values increased with time for all chitosan-GS hydrogel samples (Figure 4c, d and Figure S3 in the Supporting Information), indicating that the cells proliferated well on these chitosan-based materials. Furthermore, all hydrogel samples demonstrated improved proliferation over the control. Different from the antibacterial behavior, the genipin concentration played an important role in affecting the osteoblastic cell adhesion and proliferation. The OD values increased as the genipin concentration increased, and the chitosan-2% genipin sample exhibited the best osteogenic activity (Figure 4 and Figures S3 in the Supporting Information). This was most likely owing to the increased cross-linking of CM-chitosan at higher genipin concentration,

which lead to decreased cationicity. Actually, the cell proliferation can be further increased by the further increasing genipin concentration (data not shown here). Proliferation study was also carried out with the HA coating substrates instead of the empty culture dish, in order to test the intended usage of the prepared materials in clinical applications such as artificial joint (Figure 4d). Similar results were obtained and the chitosan samples demonstrated improved cell proliferation regardless of the substrate used. Overall, it was clear that the prepared hydrogels were even beneficial for the proliferation and adhesion of the osteoblastic cells. Although it is generally believed that the biocompatibility of chitosan lies on its interaction with anionic glycosaminoglycans (GAG) and other negatively charged molecules,³⁷ our results suggest that the positively charged chitosan might be in favor of attracting cell through electrostatic interaction, resulting in enhanced cell adhesion and proliferation.

More interestingly, the CM-chitosan materials also significantly enhanced the osteogenic differentiation of MC3T3-E1 cells, as indicated by the Runx2 and ALP measurements (Figure 4e, f and Figure S3 in the Supporting Information). As to the influence of genipin concentration, similar trend has been observed in cell differentiation as that in cell adhesion and proliferation. The expression levels of ALP and Runx2 (Figure 4e, f and Figure S3 in the Supporting Information) increased as the genipin concentration increased. Taken together, the results suggested that the higher degree of chitosan cross-linking was beneficial for the osteoblastic cell responses.

In conclusion, chitosan-GS hydrogel materials could achieve superb antibacterial efficiency and enhanced osteoblastic cell response simultaneously. We have previously reported that CM-chitosan may achieve combined antibacterial and osteogenic activities, by selectively killing the bacterial at a given concentration window.²⁵ To overcome the drawback of the suppressed antibacterial efficiency, we have adopted CM-chitosan in the hydrogel form in this study to further incorporate antibiotics, which has been routinely administered during implant surgeries. Genipin, a natural derivative of garden products with significantly less cytotoxicity compared to glutaraldehyde,³⁸ was chosen as the cross-linking agent to achieve the sustained release of the antibiotics. Our results indicated that the prepared CM-chitosan hydrogel likely selectively damaged the bacteria while attracted the osteoblastic cells. To further investigate the disrupting effect of prepared hydrogels on bacteria and cell membranes (walls), we measured the leakage of the cytoplasmic materials from *S. aureus* and MC3T3-E1 cells.

We have tested the leakage of the ALP, G6PDH, and nucleotides from *S. aureus*, to examine the disruption of the bacterium wall and membrane, respectively. The leakages of the analyzed enzymes and nucleotides gradually increased with the increase of culture time (Figure 5a–c), suggesting ongoing antibacterial activities. Overall, all synthetic materials showed higher leakages of enzymes and nucleotides than those of the blank control, indicating clear damaging effect of the synthetic hydrogel on bacterium wall/membrane. Moreover, the results suggested a weak dependence of antibacterial efficacy on genipin concentration. The leakages of the nuclear and cytoplasmic materials increased as the genipin concentration decreased, and overall the chitosan-0.5% genipin hydrogel exhibited the largest leakages of enzymes and nucleotides.

For the disruption of the cell membrane, we have examined the LDH activity in the supernatant from the MC3T3-E1 cells

(Figure 6a). The observed reduced LDH levels of the chitosan-GS hydrogels over the control suggested that the synthetic materials were even beneficial for the preservation of the cell membrane integrity. This was consistent with the proliferation study of the MC3T3-E1 osteoblasts (Figure 4c). The fluorescence staining for MC3T3-E1 (Figure 6b) further demonstrated excellent cell compatibility of the chitosan-based samples, with very little dead cells observed. Genipin's concentration also demonstrated a profound effect on the leakage of LDH and the chitosan-2% genipin sample exhibited the least leakage. Overall, the results clearly indicated the excellent selectivity of the prepared chitosan-GS hydrogels on disruption of bacteria wall/membrane over the osteoblastic cell membrane.

To investigate the influence of antibiotics (GS) on antibacterial efficacy and osteoblast response, we have performed additional experiments using chitosan-2% genipin sample with various GS loadings (Figure 7). The results suggested that the increase of the GS concentration was beneficial for both bacteria inhibition from 1 $\mu\text{g}/\text{mL}$ to 100 $\mu\text{g}/\text{mL}$ (Figure 7a) and MC3T3-E1 proliferation throughout the concentration range (Figure 7b). It was surprising to observe that the GS promoted the MC3T3-E1 cell proliferation (Figure 7b). This was likely partly due to the interaction of the hydroxyl group in GS with the amino group in chitosan, leading to the decreased availability of positive charged amino groups. The addition of the GS into CM-chitosan hydrogel was proved to be highly cytocompatible and could dramatically improve the antibacterial efficacy, which was critical for the observed excellent dual-functions of the prepared materials.

The balance of antibacterial efficacy and avoiding side effect on cell toxicity has been a challenging task for bone implant applications. Although the excellent antibacterial efficacy of the CM-chitosan hydrogel is not surprising due to the incorporation of the gentamycin sulfate, the sample also demonstrates superior osteoblastic cell response. The osteoblastic response of the chitosan hydrogel would depend on many variables, including chitosan concentration,²⁵ as well as chitosan parameters including molecular weight and degree of deacetylation, thus demonstrating potential for further optimization. More interestingly, our results suggest that both the genipin concentration and GS concentration exert a strong modulation effect on the cytocompatibility and can be used to tune and further enhance the osteoblastic cell responses. This is likely due to the cationicity of the chitosan can be modified as a result of degree of cross-linking and the interactions with its positively charged amino groups, as cationicity is critical for both antibacterial efficacy and biocompatibility.²⁶ Overall, the dual-functioned chitosan-GS hydrogel is an excellent candidate for implant materials, demonstrating great potential for integrating the antibacterial function and the osteogenic activity simultaneously.

5. CONCLUSION

In this study, we have successfully developed the dual-functioned CM-chitosan-GS hydrogels with the combined antibacterial and osteogenic activities. The chitosan-GS hydrogel had demonstrated both superb antibacterial efficacy against bacteria growth and biofilm formation of *S. aureus* and enhanced osteoblastic cell adhesion, proliferation and differentiation. The leakage of the cellular substances from various cell locations indicated the selective damage of the bacteria wall/membrane over the osteoblast membrane. The genipin

concentration not only had a profound effect on controlling the degradation time and drug release behavior of the CM-chitosan hydrogel, but also significantly affected the MC3T3-E1 cell response. The GS concentration also demonstrated a surprising modulation effect on the osteoblastic cell responses. As a result, the cell compatibility of the prepared chitosan-GS hydrogel could be tuned with both the genipin and GS concentrations. Overall, our results suggest that chitosan-based hydrogels have great potential in orthopedic applications, with combined superb antibacterial efficacy and enhanced osteogenic activity.

■ ASSOCIATED CONTENT

Supporting Information

UV-vis spectra of the relevant reaction; in vitro drug release kinetics of GS from CM-chitosan hydrogels; SEM micrograph showing osteoblastic cell adhesion; osteoblastic cell differentiation under the osteogenic induction medium. This material is available free of charge via the Internet at <http://pubs.acs.org>.

■ AUTHOR INFORMATION

Corresponding Author

*E-mail: fangwu0808@yahoo.com or fwu@scu.edu.cn. Tel.: +86 28 8541 2923. Fax: +86 28 8541 0246.

Notes

The authors declare no competing financial interest.

■ ACKNOWLEDGMENTS

We appreciate the helpful discussion with professor Bin He at Sichuan University. The study was supported by the National Basic Research program (2012cb619103), National Support Program for Science and Technology (2012BAI17B06), Natural Science Foundation grants (81271702 and 31170922), and Program for New Century Excellent Talents in University (NCET-12-0387).

■ ABBREVIATIONS

GS, gentamycin sulfate
CM-chitosan, carboxymethyl-chitosan
RGD, Arg-Gly-Asp peptide
S. aureus, *Staphylococcus aureus*
PBS, phosphate buffered saline
MTT, methyl thiazolyl tetrazolium
DMSO, dimethyl sulfoxide
OD, optical density
SEM, scanning electron microscope
HA, hydroxyapatite
FBS, fetal bovine serum
ELISA, enzyme-linked immunosorbent assay
Runx2, runt-related transcription factor-2
ALP, alkaline phosphatase
TPN, triphosphopyridine nucleotide
G6PDH, glucose-6-phosphate dehydrogenase
LDH, lactate dehydrogenase
FDA, fluorescein diacetate
PI, propidium iodide
CLSM, confocal laser scanning microscope
GAG, glycosaminoglycans

■ REFERENCES

- (1) Hetrick, E. M.; Schoenfisch, M. H. Reducing Implant-Related Infections: Active Release Strategies. *Chem. Soc. Rev.* **2006**, *35*, 780–789.
- (2) Gristina, A. G.; Oga, M.; Webb, L. X.; Hobgood, C. D. Adherent Bacterial Colonization in the Pathogenesis of Osteomyelitis. *Science* **1985**, *228*, 990–993.
- (3) Smith, A. W. Biofilms and antibiotic therapy: Is There a Role for Combating Bacterial Resistance by the Use of Novel Drug Delivery Systems? *Adv. Drug Delivery Rev.* **2005**, *57*, 1539–1550.
- (4) Chernousova, S.; Epple, M. Silver as Antibacterial Agent: Ion, Nanoparticle, and Metal. *Angew. Chem., Int. Ed.* **2013**, *52*, 1636–1653.
- (5) Hernández-Sierra, J. F.; Ruiz, F.; Cruz Pena, D. C.; Martínez-Gutiérrez, F.; Martínez, A. E.; de Jesús Pozos Guillén, A.; Tapia-Pérez, H.; Martínez Castañón, G. The Antimicrobial Sensitivity of *Streptococcus mutans* to Nanoparticles of Silver, Zinc Oxide, and Gold. *Nanomedicine* **2008**, *4*, 237–240.
- (6) Vik, H.; Andersen, K. J.; Julshamn, K.; Todnem, K. Neuropathy Caused by Silver Absorption from Arthroplasty Cement. *Lancet* **1985**, *1*, 872.
- (7) Smith, A. M.; Duan, H.; Rhyner, M. N.; Ruan, G.; Nie, S. A Systematic Examination of Surface Coatings on the Optical and Chemical Properties of Semiconductor Quantum Dots. *Phys. Chem. Chem. Phys.* **2006**, *8*, 3895–3903.
- (8) Duan, H.; Nie, S. Cell-Penetrating Quantum Dots Based on Multivalent and Endosome Disrupting Surface Coatings. *J. Am. Chem. Soc.* **2007**, *129*, 3333–3338.
- (9) Xia, T.; Kovoichich, M.; Liang, M.; Meng, H.; Kabehie, S.; George, S.; Zink, J. I.; Nel, A. E. Polyethyleneimine Coating Enhances the Cellular Uptake of Mesoporous Silica Nanoparticles and Allows Safe Delivery of siRNA and DNA Constructs. *ACS Nano* **2009**, *3*, 3273–3286.
- (10) Zasloff, M. Antimicrobial Peptides of Multicellular Organisms. *Nature* **2002**, *415*, 389–395.
- (11) Bagheri, M.; Beyermann, M.; Dathe, M. Immobilization Reduces the Activity of Surface-Bound Cationic Antimicrobial Peptides with No Influence upon the Activity Spectrum. *Antimicrob. Agents Chemother.* **2009**, *53*, 1132–1141.
- (12) Kenawy, E. R.; Worley, S. D.; Broughton, R. The Chemistry and Applications of Antimicrobial Polymers: A State-of-the-Art Review. *Biomacromolecules* **2007**, *8*, 1359–1384.
- (13) Jiang, Y.; Yang, X.; Zhu, R.; Hu, K.; Lan, W.-W.; Wu, F.; Yang, L. Acid-Activated Antimicrobial Random Copolymers: A Mechanism-Guided Design of Antimicrobial Peptide Mimics. *Macromolecules* **2013**, *46*, 3959–3964.
- (14) Chua, P.-H.; Neoh, K.-G.; Kang, E.-T.; Wang, W. Surface Functionalization of Titanium with Hyaluronic Acid/Chitosan Polyelectrolyte Multilayers and RGD for Promoting Osteoblast Functions and Inhibiting Bacterial Adhesion. *Biomaterials* **2008**, *29*, 1412–1421.
- (15) Zhang, F.; Zhang, Z.; Zhu, X.; Kang, E.-T.; Neoh, K.-G. Silk-Functionalized Titanium Surfaces for Enhancing Osteoblast Functions and Reducing Bacterial Adhesion. *Biomaterials* **2008**, *29*, 4751–4759.
- (16) Hu, X.; Neoh, K.-G.; Shi, Z.; Kang, E.-T.; Poh, C.; Wang, W. An *In Vitro* Assessment of Titanium Functionalized with Polysaccharides Conjugated with Vascular Endothelial Growth Factor for Enhanced Osseointegration and Inhibition of Bacterial Adhesion. *Biomaterials* **2010**, *31*, 8854–8863.
- (17) Shi, Z.; Neoh, K. G.; Kang, E. T.; Wang, W. Antibacterial and Mechanical Properties of Bone Cement Impregnated with Chitosan Nanoparticles. *Biomaterials* **2006**, *27*, 2440–2449.
- (18) Ong, S.-Y.; Wu, J.; Moochhala, S. M.; Tan, M.-H.; Lu, J. Development of a Chitosan-Based Wound Dressing with Improved Hemostatic and Antimicrobial Properties. *Biomaterials* **2008**, *29*, 4323–4332.
- (19) Di Martino, A.; Sittlinger, M.; Risbud, M. V. Chitosan: A Versatile Biopolymer for Orthopaedic Tissue-Engineering. *Biomaterials* **2005**, *26*, 5983–5990.
- (20) Khor, E.; Lim, L. Y. Implantable Applications of Chitin and Chitosan. *Biomaterials* **2003**, *24*, 2339–2349.
- (21) Yang, L.-q.; Lan, Y.-q.; Guo, H.; Cheng, L.-z.; Fan, J.-z.; Cai, X.; Zhang, L.-m.; Chen, R.-f.; Zhou, H. -s. Ophthalmic Drug-Loaded N, O-carboxymethyl Chitosan Hydrogels: Synthesis, *In Vitro* and *In Vivo* Evaluation. *Acta Pharmacol. Sin.* **2010**, *31*, 1625–1634.
- (22) Chung, Y.-C.; Chen, C.-Y. Antibacterial Characteristics and Activity of Acid-Soluble Chitosan. *Bioresour. Technol.* **2008**, *99*, 2806–2814.
- (23) Freier, T.; Koh, H. S.; Kazazian, K.; Shoichet, M. S. Controlling Cell Adhesion and Degradation of Chitosan Films by N-acetylation. *Biomaterials* **2005**, *26*, 5872–5878.
- (24) Gaharwar, A. K.; Schexnailder, P. J.; Jin, Q.; Wu, C.-j.; Schmidt, G. Addition of Chitosan to Silicate Cross-Linked PEO for Tuning Osteoblast Cell Adhesion and Mineralization. *ACS Appl. Mater. Interfaces* **2010**, *2*, 3119–3127.
- (25) Song, L.; Gan, L.; Xiao, Y.-F.; Wu, Y.; Wu, F.; Gu, Z.-W. Antibacterial Hydroxyapatite/Chitosan Complex Coatings with Superior Osteoblastic Cell Response. *Mater. Lett.* **2011**, *65*, 974–977.
- (26) Li, P.; Poon, Y. F.; Li, W.; Zhu, H.-Y.; Yeap, S. H.; Cao, Y.; Qi, X.; Zhou, C.; Lamrani, M.; Beuerman, R. W.; Kang, E.-T.; Mu, Y.; Li, C. M.; Chang, M. W.; Jan Leong, S. S.; Chan-Park, M. B. A Polycationic Antimicrobial and Biocompatible Hydrogel with Microbe Membrane Suctioning Ability. *Nat. Mater.* **2011**, *10*, 149–156.
- (27) Zheng, L.-Y.; Zhu, J.-F. Study on Antimicrobial Activity of Chitosan with Different Molecular Weights. *Carbohydr. Polym.* **2003**, *54*, 527–530.
- (28) Tunney, M. M.; Brady, A. J.; Buchanan, F.; Newe, C.; Dunne, N. J. Incorporation of Chitosan in Acrylic Bone Cement: Effect on Antibiotic Release, Bacterial Biofilm Formation and Mechanical Properties. *J. Mater. Sci.: Mater. Med.* **2008**, *19*, 1609–1615.
- (29) Teller, M.; Gopp, U.; Neumann, H. G.; Kühn, K. D. Release of Gentamicin from Bone Regenerative Materials: An *In Vitro* Study. *J. Biomed. Mater. Res., Part B* **2007**, *81B*, 23–29.
- (30) Baro, M.; Sánchez, E.; Delgado, A.; Perera, A.; Évora, C. *In Vitro*–*In Vivo* Characterization of Gentamicin Bone Implants. *J. Controlled Release* **2002**, *83*, 353–364.
- (31) Changez, M.; Burugapalli, K.; Koul, V.; Choudhary, V. The Effect of Composition of Poly(Acrylic Acid)–Gelatin Hydrogel on Gentamicin Sulphate Release: *In Vitro*. *Biomaterials* **2003**, *24*, 527–536.
- (32) Campos, M. N.; Rawls, H.; Innocentini-Mei, L.; Satsangi, N. *In Vitro* Gentamicin Sustained and Controlled Release from Chitosan Cross-Linked Films. *J. Mater. Sci.: Mater. Med.* **2009**, *20*, 537–542.
- (33) Teo, E. Y.; Ong, S.-Y.; Chong, M. S. K.; Zhang, Z. Y.; Lu, J.; Moochhala, S.; Ho, B.; Teoh, S.-H. Polycaprolactone-Based Fused Deposition Medoled Mesh for Delivery of Antibacterial Agents to Infected Wounds. *Biomaterials* **2011**, *32*, 279–287.
- (34) Shutipen, B.; Monnipha, S. -a.; Narong, B.; Ahnond, B. *In Vitro* Osteogenesis from Human Skin-Derived Precursor Cells. *Dev., Growth Differ.* **2006**, *48*, 263–269.
- (35) Chen, C. Z.; Cooper, S. L. Interactions Between Dendrimer Biocides and Bacterial Membranes. *Biomaterials* **2002**, *23*, 3359–3368.
- (36) Huo, K.; Zhang, X.; Wang, H.; Zhao, L.; Liu, X.; Chu, P. K. Osteogenic Activity and Antibacterial Effects on Titanium Surfaces Modified with Zn-Incorporated Nanotube Arrays. *Biomaterials* **2013**, *34*, 3467–3478.
- (37) Lee, D. W.; Lim, H.; Chong, H. N.; Shim, W. S. Advances in Chitosan Material and its Hybrid Derivatives: A Review. *Open Biomater. J.* **2009**, *1*, 10–20.
- (38) Sung, H.-W.; Huang, R.-N.; Huang, L. L. H.; Tsai, C.-C. *In Vitro* Evaluation of Cytotoxicity of a Naturally Occurring Cross-Linking Reagent for Biological Tissue Fixation. *J. Biomater. Sci., Polym. Ed.* **1999**, *10*, 63–78.